APPLICATION OF THE TIME TRANSFORMATION METHOD FOR A DETAILED ANALYSIS OF MULTISTAGE BLADE ROW INTERACTIONS IN A SHROUDED TURBINE

B. Winhart - D. Micallef - D. Engelmann

Ruhr-Universität Bochum, Chair of Thermal Turbomachinery, 44801, Bochum, Germany,
benjamin.winhart@rub.de

ABSTRACT

Transient blade loading caused by the interaction of different blade rows is one limiting factor of turbo machinery blading lifetime especially when it leads to forced response. In order to reduce the calculation effort associated with 3D computational fluid dynamics (CFD), modern transient blade row methods such as the time transformation (TT) method are used. This paper investigates the capability of the TT method to predict these phenomena by the example of the last two stages of a shrouded 4-stage air-turbine. Numerical simulations are performed using the commercial flow solver ANSYS CFX. In a detailed time step and grid influence study the sufficient resolution of all predominant flow features is ensured. The results of the TT method are then compared to a reference (REF) calculation using direct periodic treatment with focus on the force signals, frequency spectra and the distribution of the first harmonic amplitude of pressure signal along the blade surface.

KEYWORDS

ROTOR STATOR INTERACTION, TIME TRANSFORMATION METHOD, TRANSIENT BLADE ROW METHODS

NOMENCLATURE

Latin Symbols

c_{ax}	m	axial chord length
F	N	force
$\widetilde{F}$	%	force fluctuation
$\widehat{F}$	%	harmonic force fluctuation amplitude
h	m	blade height
Ma	-	Mach number
$\dot{m}$	kg/s	mass flow
n	rpm	shaft speed
p	Pa	static pressure
Re	-	Reynolds number
r	m	radial coordinate
$\bar{s}$	J/K	time & circ. averaged entropy
z	m	axial coordinate

Greek Symbols

η	-	efficiency
Π	-	pressure ratio
τ_S	s	stator passing time
$\widehat{\phi}_n$	-	n^{th} harmonic amplitude
$\check{\phi}_n$	-	n^{th} Fourier coefficient
ω	rad/s	rotational speed

Abbreviations

BC	boundary condition
DFT	discrete Fourier transformation
iDFT	inverse discrete Fourier transformation
IGV	inlet guide vane
PS	pressure side
PT	profile-transformation
RANS	Reynolds-averaged Navier-Stokes
REF	reference
SS	suction side
SST	shear stress transport
TRS	transient rotor-stator
TT	time transformation

INTRODUCTION

Due to the quick acceleration in the renewable energy market in the last decade and the subsequent change in the whole energy sector, there is a growing demand for smaller, more flexible steam turbines, which can provide a wide range of operation. The ability to precisely predict complex flow phenomena and interactions even in strong off-design conditions is essential with regard to operational safety and blading lifetime. One limiting factor for these aspects are transient blade-loadings which are mainly caused by the interactions between different blade rows. These interactions lead to time-dependent pressure fluctuations along the blade surface and thus to unsteady blade forces. Hence, there is an urgent need for an improved understanding and the ability to precisely predict these phenomena over the whole range of operation.

One way to quantify time dependent blade loadings is the application of time accurate CFD simulations. Unfortunately they require a considerable cost of computation time, due to the mostly uneven blade numbers of adjacent blade rows and the subsequent need to model multiple passages up to the whole annulus. In case of multistage simulations the computational cost increases dramatically. One way to approach this problem is the use of time accurate pitch-change methods which allow capturing the flow field of the full annulus by modeling only one or a few passages per blade row. The time transformation (TT) method is the main focus of the current investigation and represents one of these transient methods. It is based on the time-inclination method of Giles (1988) and is also applicable to multistage configurations.

In the literature the TT method has shown very promising results in terms of predicting turbo machinery performance data as Biesinger *et al.* (2010) demonstrated by the example of a one stage case (inlet guide vane (IGV) and rotor) of the 1.5 stage transonic Purdue compressor and later on the full 1.5-stage case (Biesinger *et al.* (2012)). Cornelius *et al.* (2013, 2014) investigated the multistage extension of the TT method on a modified 2.5-stage version of the 4-stage axial Hannover Compressor and a Siemens 6-stage axial compressor rig ("PCO Rig"). The performance data revealed very good correlation with the experimental data and numerical reference calculations. They further showed that dominant frequencies are transported along several blade rows but observed the existence of erroneous frequencies and amplitudes caused by the highly varying number of blades in the different blade rows. Investigating a modified Purdue 1.5-stage compressor (modified for unequal pitch of all three blade rows) Zori *et al.* (2015) showed the capability of the TT method to predict the compressor aerodynamic performance compared to a numerical reference calculation. In addition, the dominant blade-passing-frequencies where captured very well for three different blade numbers.

In this work the last two stages of a shrouded 4-stage air-turbine, located at the Chair of Thermal Turbomachinery of Ruhr-Universität Bochum are numerically investigated using the commercial flow solver ANSYS CFX release 16.1. Although it is a two stage case it is only quasi multistage due to the same blade numbers in both stator rows and both rotor rows respectively. In contrast to the aforementioned studies the focus of this work is to assess the ability of the TT method to accurately predict the excitation of the turbine blading regarding amplitudes and blade passing frequencies. To achieve this, a detailed grid influence and time step study is carried out to ensure a sufficient resolution of the predominant flow phenomena such as wakes, vortex shedding and potential effects. The results of the TT method are then compared to a reference calculation with direct periodicity treatment in terms of computation time, convergence behaviour and unsteady blade forces. To assess the quality of the results a detailed analysis of the force signals, frequency spectra and the distribution of the first harmonic amplitude of pressure signal along the blade surface is presented and compared to the reference solution.

TEST CASE

The underlying test case is a scaled 4-stage axial air-turbine test rig (Figure 1) located at the Chair of Thermal Turbomachinery of Ruhr-Universität Bochum. The test rig is currently under reconstruction as it is prepared with new measurement technology. For this reason there are no experimental data available for validation purposes yet, but are planned for future publications. The turbine is equipped with a typical high pressure blading with a constant reaction level of approximately 50 %. The last two stages are the relevant stages for the planned measurements as they are provided with milled shrouds in all four blade rows. The air is supplied by a 3-stage 3.3 MW gear compressor providing a mass flow rate of $\dot{m} \approx 12.5\,\mathrm{kg/s}$ at a pressure ratio of $\Pi \approx 2.7$. The test rig is equipped with radial and circumferential adjustable 5-hole and temperature probes in the relevant last two stages. In order to capture the interaction between the blade rows and to quantify the transient blade loadings one stator vane in the last two stages is getting equipped with high frequency, flush mounted pressure taps. The basic test rig data at the design point are shown in Table 1.

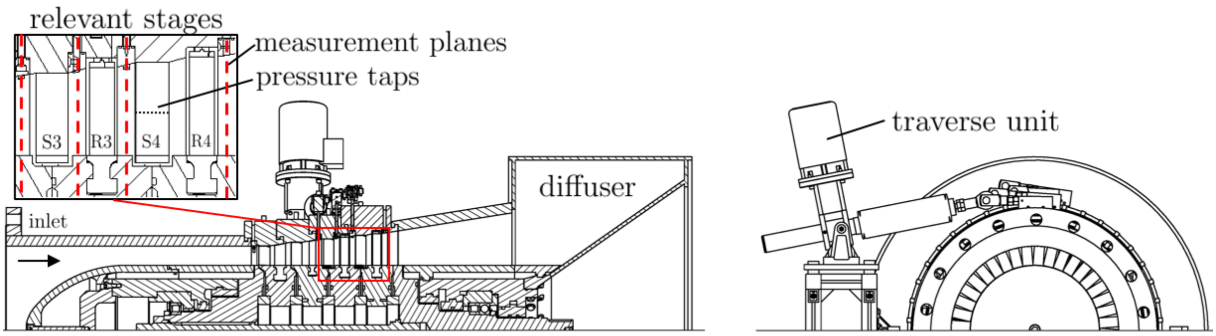

Fig. 1: **Sectional views of the turbine test rig**

		Stage 3		Stage 4	
		S3	R3	S4	R4
massflow	$\dot{m}$ [kg/s]		12.5		
shaft speed	n [rpm]	-	7000	-	7000
No. of blades	-	40	56	40	56
Reynolds no.	$Re, \cdot 10^5$	2.3	1.7	2.1	1.6
Mach no.	Ma	0.19	0.20	0.21	0.23

Table 1: **Machine data at design point**

SOLUTION METHOD

The calculations presented in this paper are performed using ANSYS CFX release 16.1. In ANSYS CFX the RANS equations are solved using a pressure-based, coupled, unstructured finite-volume algorithm (Schneider (1987)). The solver is implicit in time using a second-order backward Euler discretization. For convergence acceleration a coupled algebraic multi-grid method is used to solve the discrete system of flow equations. All steady and unsteady simulations where performed using the shear stress transport (SST) two equation turbulence model, developed by Menter (1994). In steady state simulations the interfaces between adjacent blade rows are treated using the mixing plane approach. In the unsteady reference simulation a transient rotor-stator interface is applied. All other calculations are done using the TT method in order to overcome unequal pitch ratios. A short description of commonly used blade row interfaces is given below.

Transient Rotor-Stator

The transient rotor-stator (TRS) model predicts the true transient interaction of the flow between adjacent blade rows. Therefore, it is required to assure that all pitch ratios are equal to one. The interface is fully implicit and conservative. The transient relative motion between the meshes of different components is updated at each time step so that this model is able to precisely resolve all interaction effects. On the downside this method has very large requirements in terms of calculation time, memory and disk space because it is mostly necessary to model multiple passages up to the full annulus.

Profile-Transformation Method

The profile-transformation (PT) method allows overcoming the unequal pitch ratios in a transient simulation by scaling the flow profiles between adjacent blade rows via an interface flux scaling procedure across the rotor-stator interface (Galpin, 1995). Therefore, only one to a few passages per blade row need to be modeled. On the circumferential interfaces a periodic boundary condition is applied. The PT method improves the performance prediction compared to the steady-state simulations as it is able to resolve the interactions between different blade rows. However, the profile scaling induces a transformation error which behaves proportional to the pitch ratio. In order to reduce this error it is possible to model additional passages, resulting in an ensemble pitch ratio close to unity. The PT method is not investigated in this work but should be mentioned as it is the basis for the TT method.

Time Transformation Method

The TT method is based on the time-inclination approach of Giles (1988), which is an advancement of the PT method. In the used solver it is implemented in a fully implicit way and is also applicable to multistage problems. The method overcomes unequal pitch ratios by inclining the time axis in order to guarantee simple periodicity in the circumferential direction. With the transformation of the full Navier-Stokes equations and the turbulence model transport equations there is no frequency error across the interface of adjacent blade rows as it occurs in the PT method. The numerical constraints of this method are its limitation to compressible flows within a certain range of pitch ratios of neighbouring blade rows. For a numerically stable simulation the pitch ratio P_S/P_R has to be in a range dependent on the Mach number associated to the rotor rotational speed Ma_ω and the Mach number associated to the circumferential velocity Ma_θ:

$$1 - \frac{Ma_\omega}{1 - Ma_\theta} < \frac{P_S}{P_R} < 1 + \frac{Ma_\omega}{1 + Ma_\theta} \qquad (1)$$

For most compressible turbo machinery applications this range of pitch ratios lies within 0.6 - 1.5 (Giles, 1988).

NUMERICAL SETUP

As described above only the last two stages of the 4-stage air-turbine test rig are modeled in order to keep the computational cost within limits. Because of the existing blade numbers of 40-56-40-56 the pitch ratio is 0.7143 or 1.4, which is out of the stable area for this case

($0.73 \leq P_S/P_R \leq 1.38$). To overcome this issue the number of blades modeled in the numerical domain is adjusted to 2-3-2-3 (Figure 2 (left)) which leads to an ensemble pitch ratio close to unity.

The passage meshes are created using ANSYS TurboGrid while the meshing of the shroud cavities is done in ANSYS ICEM. The interfaces between the passages and the cavities are realized using a frozen rotor interface.

For the inlet boundary condition (BC) the distribution of total pressure, total temperature and the flow direction is extracted from a one passage, steady state, mixing plane calculation of the whole machine which is extended to two passages (Figure 2 (left)). At the outlet an averaged static pressure BC is imposed.

All unsteady runs are performed for a single rotor revolution with a convergence criterion of $\mathcal{R}_{\max} \leq 5 \cdot 10^{-3}$ for all residuals.

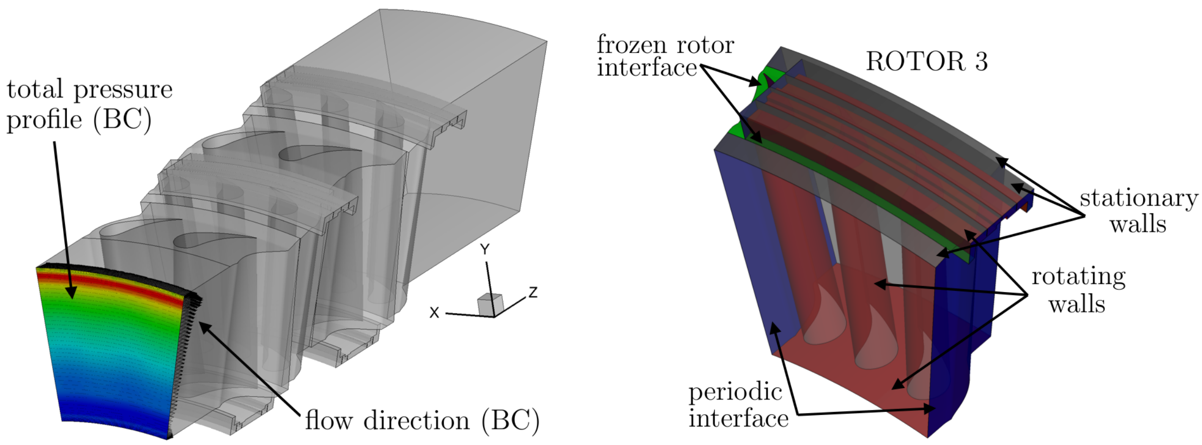

Fig. 2: **Computational domain with inlet distribution of total pressure BC and velocity vectors (left); Boundary conditions for one blade row (right)**

POST-PROCESSING PROCEDURE

In case of using the TT method the flow variables are transformed into the frequency domain. Therefore Fourier coefficients are accumulated during the simulation via a discrete Fourier transformation (DFT):

$$\check{\phi}[k] = \frac{1}{N} \sum_{n=0}^{N-1} \phi[n] e^{-j\frac{2\pi}{N}nk}. \tag{2}$$

This procedure makes it possible to reconstruct the time inclined data back to the physical time. For the data output only one file is generated containing all specified Fourier coefficients for the desired variables. This results in less disk-space usage since it is not necessary to save transient field data for every time step. For post-processing the data, an external environment was developed by the authors (Figure 3) which contains the following basic components:

- **sort profile data:** This routine rearranges the unstructured data output. The data is sorted by radius and divided into suction side and pressure side.

- **force signals:** This routine provides all force components. In case of TT data output the force signals are retransformed into the time domain using an inverse discrete Fourier transformation (iDFT):

$$\phi[n] = \sum_{k=0}^{N-1} \check{\phi}[k] e^{j\frac{2\pi}{N}nk}. \tag{3}$$

- **frequency spectra:** In this routine the frequency spectra are computed from the force signals using a DFT. In order to get sharp spectra it is important that the chosen time step in the force reconstruction module fits into the beating period as an integer value.
- **harmonic amplitudes:** In case of TT data output the distribution of different harmonic amplitudes is directly visualized using the sorted Fourier coefficients along the blade surface. For the REF data output the pressure signals of every point along the blade surface has to be transformed into the frequency domain using Eq. 2.

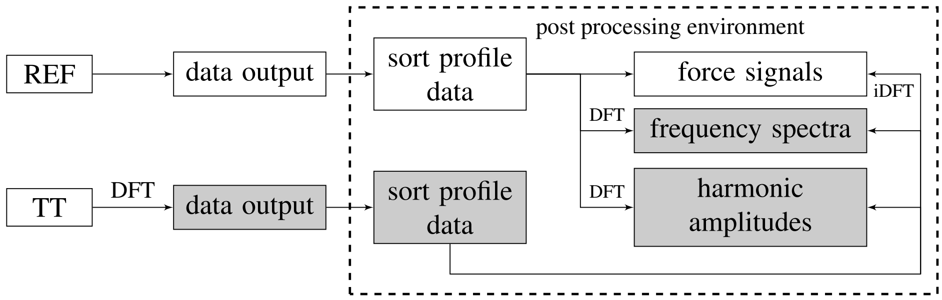

Fig. 3: **Process describing the post processing procedure; white: time domain data; grey: frequency domain data**

TIMESTEP & GRID INFLUENCE STUDY

In order to guarantee a sufficient spatial and temporal resolution of all flow phenomena which are important for the rotor-stator interaction, a detailed time step & grid influence study is performed. This study is carried out using the TT method to keep the computational effort within limits. For the grid influence study three different meshes are generated using ANSYS TurboGrid. The main difference between these meshes is their resolution in the blade-to-blade area as well as in span-wise direction. The resolution of the blade boundary layers is only slightly modified to avoid adverse aspect ratios ($y^+ \approx \mathcal{O}(1)$). The resolution of the hub and shroud boundary layers is kept constant, as well as the resolution of the leakage mesh. Table 2 (left) summarizes the basic data of the three grids. The considered time steps are listed in Table 2 (right). For the sake of improved clarity the time step study is only shown for the final grid and the grid influence study only for the final time step. The other combinations show similar behaviour.

Timestep Study

The influence of the time step resolution is examined in terms of the unsteady blade forces and the frequency spectra of the blade force signals. Figure 4 (left) shows the force fluctuations

	Total	S3	R3	S4	R4
Coarse	3.08M	252.8K	183K	272.8K	250.5K
Medium	**5.44M**	**545.2K**	**389.8K**	**532.1K**	**463K**
Fine	10.27M	1123K	765.4K	1080K	947.2K

	$\tau_S/\Delta t$ [-]	$\Delta t, \cdot 10^{-6}$ [s]
no. of timesteps	32	6.69644
	64	**3.34822**
	128	1.67411

Table 2: **Number of elements per passage and for the whole modeled domain (left); Timestep sizes (right)**

over five stator passing periods for the final grid B. The curves representing 64 and 128 time steps per stator blade passing indicate a very good accordance, whereas the 32 time steps curve shows a large deviation. The frequency spectra of the force signals are given in Figure 4 (right). It can be observed that mostly the first two harmonics are predominant. The largest difference is given in the frequency spectrum of stator 4 where the amplitudes of the first 2 harmonics belonging to the 32 time step case differ widely. Although the force signals and frequency spectra of the 64 and 128 time steps case show slight differences, especially in the second harmonic of rotor 4, 64 time steps are picked for further calculations as an acceptable compromise between accuracy and computational cost.

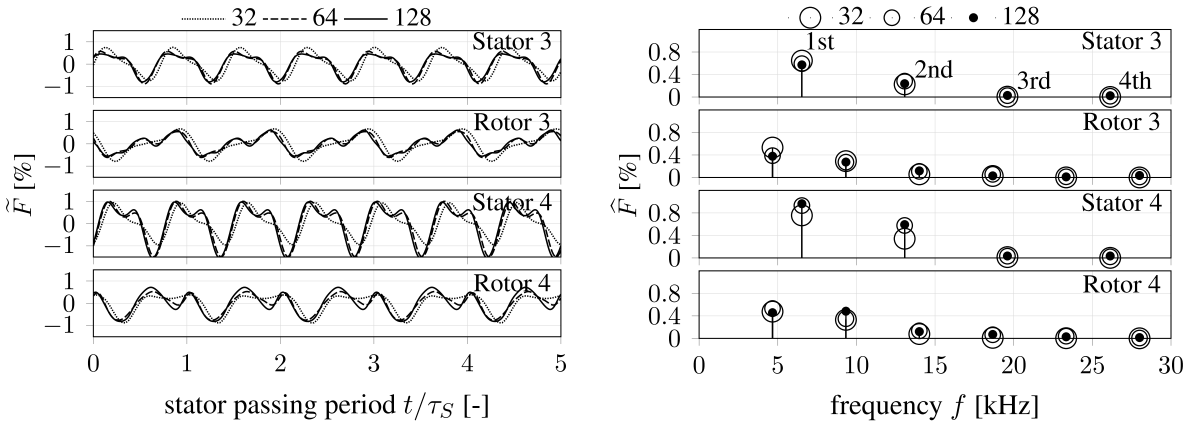

Fig. 4: **Force fluctuations over stator passing period (left); Frequency spectra of the force signals (right)**

Grid Influence Study

As given in Figure 5 the influence of the numerical grid is examined the same way as in the time step study. It is found that the influence of the grid resolution has a very small impact on the force signal of the first stator row. This is due to the fact that the unsteady blade force of stator 3 is only affected by the potential field of the following rotor, which is obviously captured very well by all numerical grids. The difference between the investigated grids increases in the other blade rows where additional wake effects are getting more relevant. In the force signal of the coarse grid an additional phase shift is observed in rotor 4, which is caused by the under turning of stator 4 due to the low resolved blade trailing edge. Although the grid influence is not as big as expected, grid A does not seem to sufficiently resolve all flow features. Grid B in contrast shows good accordance to Grid C and is therefore chosen for further simulations.

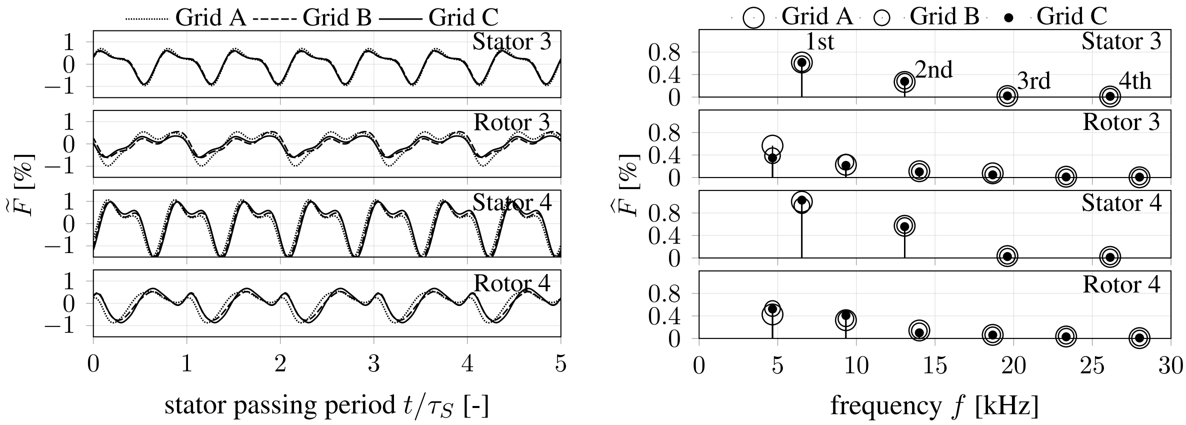

Fig. 5: **Force fluctuations over stator passing period (left); Frequency spectra of the force signals (right)**

NUMERICAL VALIDATION

The results obtained using the TT method on the final grid using 64 time steps per stator blade passing is validated against a reference calculation using direct periodic treatment. In case of the existing blade numbers the reference calculation is realized by a 45 degree segment simulation which results in a total element count of 13.1 million elements.

Force Signals & Spectra

In case of the reference simulation the force signals are computed using time exact transient data output. The signals are shown in Figure 6 together with the corresponding frequency spectra. Both data sets indicate an overall good agreement with slight deviations in the amplitudes of certain harmonics. This is mainly caused by some low frequent harmonic content superposing the signals in case of the reference calculation which could be imposed by the $45°$-segment simulation and may not occur in a full wheel simulation. To reduce this effect the signals are phase-averaged over the last blade passing periods.

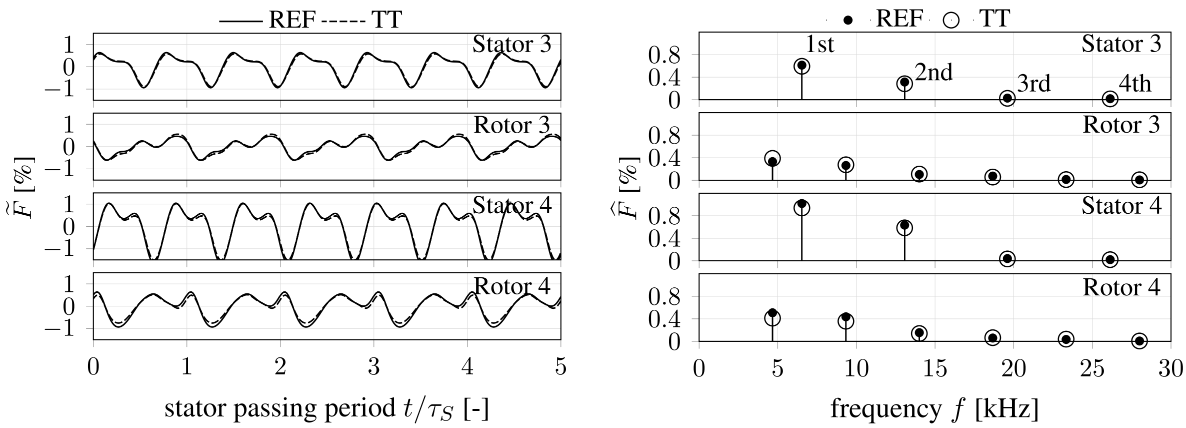

Fig. 6: **Force fluctuations over stator passing period (left); Frequency spectra of the force signals (right)**

Harmonic Amplitudes

In order to gain a better understanding of the flow phenomena causing these differences, the distribution of the first harmonic pressure amplitude

$$\widehat{p}_1 = \sqrt{\Re(\check{p}_1)^2 + \Im(\check{p}_1)^2} \tag{4}$$

along the blade surfaces is examined. In case of the reference calculation the time exact data output is transformed into the frequency domain for every surface element on the blades using the DFT algorithm given in Equation (2). Figure 7 shows contours of the first harmonic amplitude along the normalized blade surface for the reference simulation (left) and the absolute variance

$$|\Delta\hat{p}| = |\hat{p}_{\mathrm{REF}} - \hat{p}_{\mathrm{TT}}| \tag{5}$$

of the TT solution compared to the reference solution (right). The distribution along the blade surface of Stator 3 shows very small amplitudes compared to the other blade rows. The highest amplitudes are located on the suction side (SS) near the trailing edge where the potential effects of rotor 3 have the highest impact. In the other blade rows the highest amplitudes are located in the front half of the suction side of the blade (Figure 7 (left)).

In Figure 7 (right) the absolute variance of TT and REF calculation is shown. It can be seen that there is a good overall accordance between these two results but there are big differences in the root region of the rotor blades. These regions are affected by the leakage flow caused by the upstream stator cavities which impinges the passage flow and leads to pressure fluctuations along the blade surface in this area. Obviously there are some issues at the interfaces between cavities and passage flow which will be discussed in the next chapter.

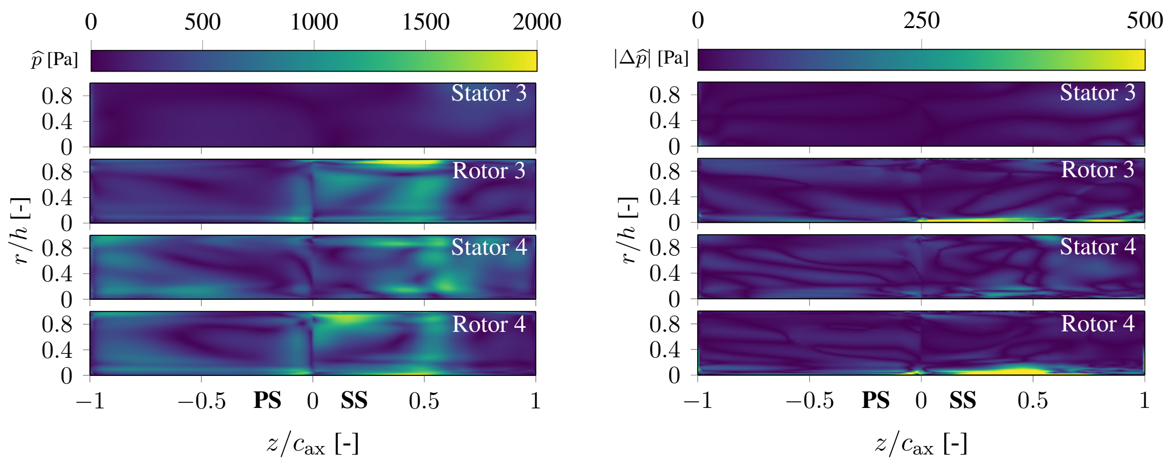

Fig. 7: **First harmonic amplitude of the pressure signal (REF) (left); absolute variance between REF and TT case (right)**

Meridional Entropy Distribution

In Figure 8 (left) the circumferential and time averaged entropy is shown in a meridional view for the reference calculation. The positions of the particular blade leading edge and trailing edge are indicated in white. In the regions of the cavities a rise of entropy can be observed due to the loss generated by the mixing process. The percentage variance between the two cases is shown in Figure 8 (right). The largest differences are in the hub regions which confirms the assumption that in the TT case the mixing process in the area of the stator cavities is not predicted correctly. Additional spectral analysis inside the cavity domains revealed that there are frequency shifts through the frozen rotor interfaces which connects the cavity domains to the passages.

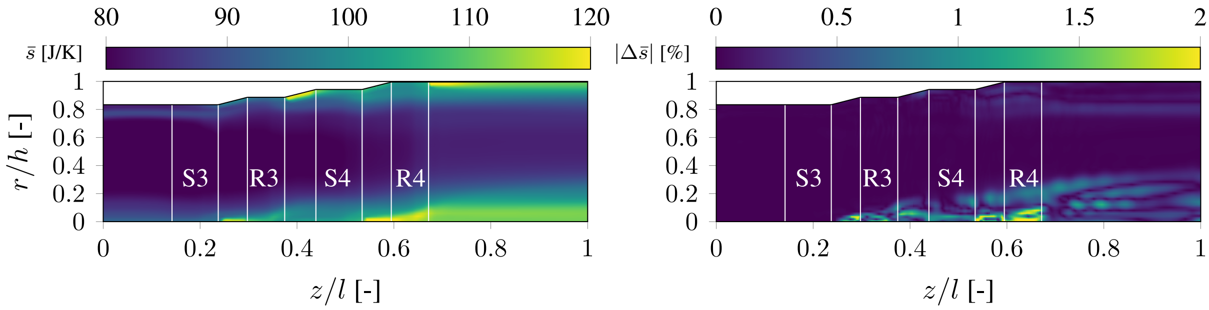

Fig. 8: **Circ. averaged entropy $\bar{s}$ for reference calculation (left); Percentage variance of $\bar{s}$ (right)**

CONVERGENCE & COMPUTATIONAL COST

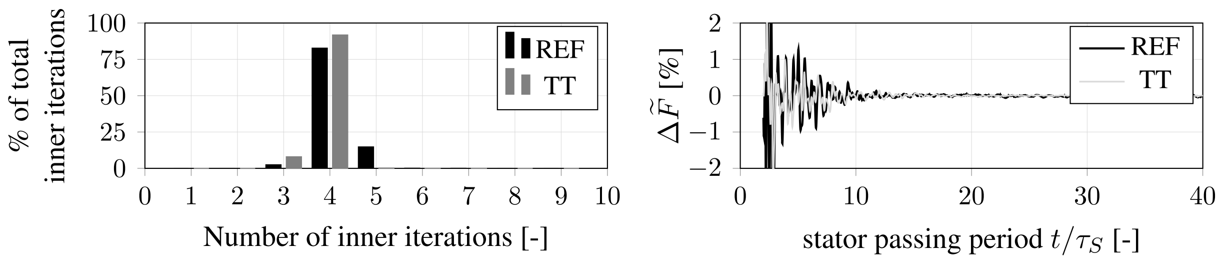

Fig. 9: **Percentage of total inner iterations (left); Convergence of Rotor 3 force signal (right)**

As mentioned before the TT method is implemented in CFX in a fully implicit manner which provides a very fast convergence behaviour. The convergence criterion of $5 \cdot 10^{-3}$ is reached at an average of 4 iterations per time step as shown in Figure 9 (left). In comparison with the reference calculation the TT method needs even less inner iterations per time step. Figure 9 (right) shows the convergence of the force signal of rotor 3 over the whole simulation process. Both simulations achieve a very fast convergence. After approximately 10 stator passing periods the moving difference described by

$$\Delta\widetilde{F}(t+\tau_S) = \frac{\widetilde{F}(t+\tau_S) - \widetilde{F}(t)}{\widetilde{F}(t)} \qquad (6)$$

stays below 0.2%. The signals of the other blade rows show similar behaviour. In terms of calculation time the TT calculation is 2.18 times faster than the REF calculation. This time advantage increases even more in case the blade numbers require a full wheel calculation. The data given in Table 3 summarize the computational effort for both cases on the final grid and time step.

method	cores	computation time	CPU hours
REF	80	1d 20h 49 min	3575
TT	80	20h 33min	1638

Table 3: **computational effort**

SUMMARY & CONCLUSION

In the present study the TT method was used to simulate the last two stages of a four stage shrouded air turbine. The aim was to assess the ability of the TT method to precisely predict the unsteady blade forces caused by the interaction of different blade rows.

In order to guarantee the spatial and temporal resolution of all relevant flow phenomena a detailed grid influence and time step study was carried out. The time step study showed that time discretization plays an important role in terms of sufficiently resolving all flow features causing the unsteady blade loadings such as wakes, potential effects and vortex shedding. It revealed that 64 time steps per stator blade passing are sufficient for this case. According to the conducted grid influence study a spacial resolution of around 480,000 elements per passage is recommendable.

The results obtained using the TT method where numerically validated against a 45 degree segment reference calculation with direct periodic treatment and compared for every blade row by unsteady force signals, frequency spectra of force signals and the distribution of first harmonic of the pressure signals along the blade surfaces. The force signals where in very good accordance to the reference simulation as well as the frequency spectra. Only slight differences could be observed at some harmonics.

The distribution of the first pressure harmonic showed an overall good accordance with some differences in the hub region of the rotor blades. It seemed logical to assume that these differences are related to the cavity flow from the upstream stator cavities. An investigation of the time- and circumferential averaged meridional distribution of the entropy proved this assumption as it showed major differences only in the region where the stator cavity flows impinge the passage flow.

The investigations showed that the TT method is capable to predict the unsteady blade forces in the last two stages of a 4-stage shrouded air turbine but causes errors at the interfaces between non inclined cavity domains and inclined passage domains. For this test case these errors do not have a strong influence on the overall forces so that the harmonic content is depicted very well compared to the reference calculation.

Additional investigations regarding the application of TT method for multi disturbance flows were conducted by the authors by including the second stage of the test rig. These results are not included in this work but looked promising compared to a reference calculation. For additional disturbances we saw erroneous frequencies coming up, like Cornelius *et al.* (2013, 2014) observed as well.

Future work deals with approaches to avoid the issues in the region of the stator cavities which are currently connected through a simple frozen rotor interface to the stator domains. One option could be a single domain meshing of cavity and passage without the use of any interface.

In addition, the size of the modeling error has to be determined which occurs caused by the reduction of the full model to a 2-stage model. Therefore, it is planned to perform a full annulus simulation of the whole 4-stage machine and to compare the obtained numerical results with future experimental data.

ACKNOWLEDGMENTS

The development work was conducted as a part of the joint research program COOREFLEX-turbo in the frame of AG Turbo. The work was supported by the Bundesministerium für Wirtschaft und Technologie (BMWi) as per resolution of the German Federal Parliament under grant number 03ET7040F. The authors gratefully acknowledge AG Turbo and MAN Diesel & Turbo SE for their support and permission to publish this paper. The responsibility for the content lies solely with its authors.

REFERENCES

Biesinger T., Cornelius C., Rube C., Schmidt G., Braune A., Campregher R., Godin P.G., Zori L. (2010), *Unsteady CFD Methods in a Commercial Solver for Turbomachinery Applications*, ASME Paper No. GT2010-22762.

Biesinger T., Cornelius C., Nürnberger D., Rube C. (2012), *Speed Line Computation of a Transonic Compressor Stage with Unsteady CFD Methods*, ASME Paper No. GT2012-68029.

Cornelius, C., Biesinger, T., Galpin, P., Braune, A. (2013), *Experimental and Computational Analysis of a Multistage Axial Compressor Including Stall Prediction by Steady and Transient CFD Methods*, ASME Paper No. GT2013-94639.

Cornelius, C., Biesinger, T., Zori, L., Campregher, R., Galpin, P., Braune, A. (2014), *Efficient Time Resolved Multistage CFD Analysis Applied to Axial Compressors*, ASME Paper No. GT2014-26846.

Galpin P.F., Hutchinson B.R. (1995), *Three Dimensional Navier-Stokes Predictions of Steady State Rotor-Stator Interaction with Pitch Change*, Third Annual Conference of the CFD Society of Canada

Menter, F. (1994), *Two-equation eddyviscosity turbulence models for engineering applications*, AIAA Journal, Vol. 23, No. 8, pp. 1598-1605.

Giles, M. (1988), *Calculation of Unsteady Wake/Rotor Interaction*, Journal of Propulsion & Power, Vol 4, No 4, pp. 356-362.

Schneider, G., Raw, M. (1987), *Control volume finite-element method for heat transfer and fluid flow using collocated variables – 1. Computational procedure*, Numerical Heat Transfer, Vol 11, No 4., pp. 363-390.

Zori, L., Galpin, P., Campregher, R., Morales, J.C. (2015), *Time Transformation Simulation of 1.5 Stage Transonic Compressor*, ASME Paper No. GT2015-43624.